Comput Mech (2005) 35: 134–145
DOI 10.1007/s00466-004-0610-0

ORIGINAL PAPER

Y. T. Gu· G. R. Liu

A meshfree weak-strong (MWS) form method for time dependent problems

Received: 15 March 2004 / Accepted: 28 June 2004 / Published online: 11 August 2004

Abstract A meshfree weak-strong (MWS) form method, which is based on a combination of both the strong form and the local weak form, is formulated for time dependent problems. In the MWS method, the problem domain and its boundary are represented by a set of distributed field nodes. The strong form or the collocation method is used to discretize the time-dependent governing equations for all nodes whose local quadrature domains do not intersect with natural (derivative or Neumann) boundaries. Therefore, no numerical integration is required for these nodes. The local weak form, which needs the local numerical integration, is only used for nodes on or near the natural boundaries. The natural boundary conditions can then be easily imposed to produce stable and accurate solutions. The moving least squares (MLS) approximation is used to construct the meshfree shape functions in this study. Numerical examples of the free vibration and dynamic analyses of two-dimensional structures as well as a typical micro-electromechanical system (MEMS) device are presented to demonstrate the effectivity, stability and accuracy of the present MWS formulation.

Keywords Computational mechanics · Numerical analysis · Meshfree method · Meshless method · Time dependent · MEMS

1 Introduction

Meshless or meshfree methods have attracted more and more attention from researchers in recent years, and are regarded as promising numerical methods for computational mechanics, as they do not require a mesh to discretize the problem domain, because the approximate solution is constructed entirely based on a set of scattered nodes. A detailed review of meshfree methods can be found in the recent monograph by Liu (2002). Current meshfree methods can be largely categorized into two major categories: meshfree methods based on strong forms (or short for meshfree strong-form methods) and meshfree methods based on weak forms (or short for meshfree weak-form methods) (Liu and Gu, 2004).

The meshfree strong-form methods usually use collocation techniques (e.g. Zhang et al., 2001) to form the system equations. They have been found to possess the following attractive advantages (Liu and Gu, 2004):

- They are truly meshless methods. No mesh is used in the whole processes.
- The procedure is basically straightforward, and hence the algorithms and coding are very simple.
- They are computationally efficient, and the solution is accurate when there are only Dirichlet boundary conditions.
- Implementation of Dirichlet boundary condition is very straightforward.

Owing to the above advantages, meshfree strong-form methods have been studied and used in computational mechanics. However, shortcomings of meshfree strong-form methods are also very obvious. In the meshfree strong-form methods, derivative (Neumann) boundary conditions are posted by a set of separate differential equations defined on the boundary, which is different from the governing equations defined in the problem domain. They are sometimes unstable and less accurate, especially for problems governed by partial differential equations (PDEs) with derivative boundary conditions, such as solid mechanics problems with stress (natural) boundary conditions. Several strategies have been developed to overcome this problem, and these techniques have been summarized in some publications (e.g. Liu GR and Gu YT, 2004).

Y. T. Gu (✉) · G. R. Liu
Centre for Advanced Computations in Engineering Science (ACES) Dept. of Mechanical Engineering, National University of Singapore,
10 Kent Ridge Crescent, Singapore 119260
E-mail: mpeguyt@nus.edu.sg

G. R. Liu
SMA Fellow, Singapore-MIT Alliance (SMA)

The common feature of meshfree weak-form methods, such as the element-free Galerkin (EFG) method (Belytschko et al., 1994), the point interpolation method (Liu and Gu, 2001a), the radial point interpolation method (RPIM) (Wang and Liu, 2002), the meshless local Petrov-Galerkin method (MLPG) (Atluri et al., 1999; Gu and Liu, 2001a), and the local radial point interpolation method (LRPIM) (Liu and Gu, 2001c), is that the PDE (strong-form) of a problem is firstly replaced by or converted into an integral equation (global or local) based on a principle (weighted residual methods, energy principle etc.). Weak-form system equations can then be derived by integral by parts. A set of system equations of meshfree weak-form methods can be obtained from the discretization of the weak-form using the meshfree interpolation techniques. The meshfree weak-form methods have the following advantages.

- They have good stability and accuracy for many problems.
- The traction (derivative or Neumann) boundary conditions can be naturally and conveniently incorporated into the same weak-form equation.
- A method developed properly using a weak-form formulation is applicable to many other problems.

Owning to these advantages, meshfree weak-form methods have been successfully applied in solid and fluid mechanics problems. However, meshfree global weak-form methods are "meshfree" only in terms of the interpolation of the field variables. Background cells have to be used to integrate a weak-form over the global problem domain. The numerical integration makes them computationally expensive, and not "truly" meshless. In order to remove the global integration background mesh, meshfree methods based on the local Petrov-Galerkin weak-forms have been proposed, such as the meshless local Petrov-Galerkin (MLPG) method (Atluri et al., 1999; Atluri and Shen, 2002), the local boundary integral equation (LBIE) method (Zhu et al., 1998), the method of finite spheres (De and Bathe, 2000), the local point interpolation method (LPIM) (Liu and Gu, 2001b; Gu and Liu, 2001c; Lam et al., 2004; Li et al., 2004), the local radial PIM (LRPIM) (Liu and Gu, 2001c; Liu and Yan et al., 2002) that developed based on the idea of MLPG, etc.

Although the meshfree local weak-form methods made a significant step in the direction of developing ideal meshfree methods, the numerical integration is still a burdensome task, especially for nodes on or near the boundaries with complex shape. The local integration can still be computationally expensive for some practical problems. It is therefore desirable to minimize the need for numerical integrations.

The meshfree strong-form methods and the meshfree local weak-form methods both have their own advantages and their own shortcomings. Hence, the combination of the strong-form and the local weak-form has been used to propose a novel meshfree method, the meshfree weak-strong (MWS) form method (Liu and Gu, 2003), and the MWS method has been used for two-dimensional elasto-statics. In this paper, a MWS formulation is developed for time dependent problems. In this MWS formulation, the problem domain and its boundary are represented by a set of distributed field nodes. The strong form or collocation method is used to discretize the time-dependent governing equations for all nodes whose local quadrature domains do not intersect with natural (derivative or Neumann) boundaries. Therefore, no numerical integration is required for these nodes. The local weak form, which needs the local numerical integration, is only used for nodes on or near the natural boundaries. The natural boundary conditions can then be easily imposed to produce stable and accurate solutions. The moving least squares (MLS) approximation is used to construct the meshfree shape functions in this study. Numerical examples of the free vibration and dynamic analyses of two-dimensional (2-D) solids and a typical microelectromechanical system (MEMS) device are presented to demonstrate the efficiency, stability and accuracy of the present MWS formulation.

2 Meshfree weak-strong (MWS) formulation for 2-D elastodynamics

The problem of elastodynamics is an important time dependent problem in computational mechanics. The strong form of the initial/boundary value problem for 2-D linear elastodynamics is as follows:

$$\sigma_{ij,j} + b_i = m\ddot{u}_i + c\dot{u}_i \tag{1}$$

where m is the mass density, c is the damping coefficient, $\ddot{u}_i = \frac{\partial^2 u_i}{\partial t^2}$ is the acceleration, $\dot{u}_i = \frac{\partial u_i}{\partial t}$ the velocity, σ_{ij} the stress tensor, which corresponds to the displacement field u_i, b_i the body force tensor, and $()_j$ denotes $\frac{\partial}{\partial x_j}$. The auxiliary conditions are given as follows:

$$\text{Natural boundary condition} \ : \ \sigma_{ij} n_j = \bar{t}_i \quad \text{on } \Gamma_t \tag{2}$$

$$\text{Essential boundary condition} : u_i = \bar{u}_i \quad \text{on } \Gamma_u \tag{3}$$

$$\text{Displacement initial condition} \ : \mathbf{u}(\mathbf{x}, t_0) = \mathbf{u}_0(\mathbf{x}) \quad \mathbf{x} \in \Omega \tag{4}$$

$$\text{Velocity initial condition} \ : \dot{\mathbf{u}}(\mathbf{x}, t_0) = \mathbf{v}_0(\mathbf{x}) \quad \mathbf{x} \in \Omega \tag{5}$$

in which the $\bar{u}_i$, $\bar{t}_i$, $\mathbf{u}_0$ and $\mathbf{v}_0$ denote the prescribed displacements, tractions, initial displacements and velocities, respectively, and n_j is the unit outward normal to the domain Ω.

As shown in Fig. 1, the problem domain and boundaries are represented by properly scattered field nodes. The key idea of the MWS method (Liu and Gu, 2003) is that in establishing the discrete system equations, both the strong form and the local weak form are used for the same problem, but for different field nodes. In Fig. 1, Ω_q is the local quadrature domain for a field node. If Ω_q does not intersect with the natural bound-

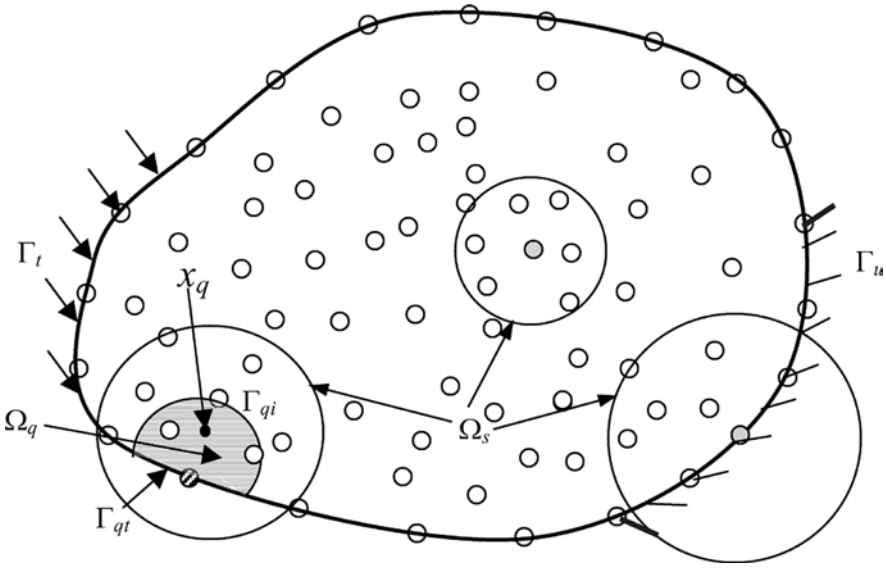

Fig. 1 Sub-domains used in the MWS method: the local support domain Ω_s , local quadrature domain Ω_q

aries, the strong form is used for this node. Otherwise, the local weak form is used.

2.1 Strong form for 2-D elastodynamics

For an internal node or a node on the essential boundary, whose local quadrature domain does not intersect with the natural boundary, equation (1) for isotropic materials can be written as the following standard strong form.

$$\begin{cases} \dfrac{E}{1-v^2}\left(\dfrac{\partial^2 u}{\partial x^2}+\dfrac{1-v}{2}\dfrac{\partial^2 u}{\partial y^2}+\dfrac{\partial^2 v}{\partial x \partial y}\right)+b_x-m\dfrac{\partial^2 u}{\partial t^2}-c\dfrac{\partial u}{\partial t}=0 \\ \dfrac{E}{1-v^2}\left(\dfrac{\partial^2 v}{\partial y^2}+\dfrac{1-v}{2}\dfrac{\partial^2 v}{\partial x^2}+\dfrac{\partial^2 u}{\partial x \partial y}\right)+b_y-m\dfrac{\partial^2 v}{\partial t^2}-c\dfrac{\partial v}{\partial t}=0 \end{cases} \tag{6}$$

where E and v are Young's modulus and Poisson ratio, u and v are displacements at x and y direction, respectively. b_x and b_y are body forces at x and y direction. The collocation method is used directly to discretize Eq. (6).

2.2 Local weak form

If Ω_q of a field node intersects with the natural boundaries, the local weak form is used (Atluri et al., 1999; Liu, 2002). A generalized local weak form of the partial differential Eq. (1), over a local quadrature domain Ω_q bounded by Γ_q, can be obtained using the weighted residual method or the local Petrov-Galerkin method (e.g., Atluri et al., 1999):

$$\int_{\Omega_q} \widehat{w}_i(\sigma_{ij,j}+b_i-m\ddot{u}_i-c\dot{u}_i)\mathrm{d}\Omega - \alpha \int_{\Gamma_{qu}} \widehat{w}_i(u_i-\bar{u}_i)\mathrm{d}\Gamma = 0 \tag{7}$$

where $\widehat{w}_{wi}$ is the weight function. It should note here that the last penalty term in (7) is to enforce the essential boundary condition. This term is necessary because MLS shape functions lack delta function properties.

The first term on the left hand side of Eq. (7) can be integrated by parts to get

$$\int_{\Gamma_q} \widehat{w}_i\sigma_{ij}n_j\mathrm{d}\Gamma + \int_{\Omega_q} [-\widehat{w}_{i,j}\sigma_{ij}+\widehat{w}_i(b_i-m\ddot{u}_i-c\dot{u}_i)]\mathrm{d}\Omega - \alpha \int_{\Gamma_{qu}} \widehat{w}_i(u_i-\bar{u}_i)\mathrm{d}\Gamma = 0 \tag{8}$$

The local quadrature domain Ω_q of a node x_i is a domain in which $\widehat{w}_i \neq 0$. An arbitrary shaped local quadrature domain can be used. A circle or rectangular quadrature domain is used in this paper for convenience. It can be found that the boundary Γ_q for the local quadrature domain usually comprises three parts: the internal boundary Γ_{qi}, the boundaries Γ_{qu} and Γ_{qt}, over which the essential and natural boundary conditions are specified. Imposing the natural boundary condition and noticing that $\sigma_{ij}n_j = \frac{\partial u}{\partial n} \equiv t_i$ into Eq. (8), the following local weak form can be obtained.

$$\int_{\Omega_q} (\widehat{w}_i m\ddot{u}_i + \widehat{w}_i c\dot{u}_i + \widehat{w}_{i,j}\sigma_{ij})\mathrm{d}x - \int_{\Gamma_{qi}} \widehat{w}_i t_i \mathrm{d}\Gamma - \int_{\Gamma_{qu}} \widehat{w}_i t_i \mathrm{d}\Gamma + \alpha \int_{\Gamma_{qu}} \widehat{w}_i u_i \mathrm{d}\Gamma = \int_{\Gamma_{qt}} \widehat{w}_i \bar{t}_i \mathrm{d}\Gamma + \alpha \int_{\Gamma_{qu}} \widehat{w}_i \bar{u}_i \mathrm{d}\Gamma + \int_{\Omega_q} \widehat{w}_i b_i \mathrm{d}\Omega \tag{9}$$

It can be seen from Eq. (9), the Neumann boundary conditions Eq. (2) have been satisfied naturally in the local weak form.

The test (weight) function plays an important role in the performance of the local weak form. Theoretically, any weight function is acceptable as long as the condition of continuity is satisfied. Many studies about the weight functions for the local weak form in the local meshfree methods have been performed (e.g., Atluri et al., 1999; Atluri and Shen,2002; Liu, 2002). In order to simplify the local weak form, we can deliberately select the test functions such that they vanish over Γ_{qi}, although it is not necessary. This can be easily satisfied using the following 4th-order spline weight function.

$$\widehat{w}_i(x) = \begin{cases} 1 - 6\left(\frac{d_i}{r_w}\right)^2 + 8\left(\frac{d_i}{r_w}\right)^3 - 3\left(\frac{d_i}{r_w}\right)^4 & 0 \le d_i \le r_w \\ 0 & d_i \ge r_w \end{cases} \tag{10}$$

where $d_i = |x_Q - x_i|$ is the distance from node x_i to point x_Q, and r_w is the size of the support for the weight function. The support radius of weight function, r_w, can be simply selected as the same size of the local quadrature domain for the local weak form. The selection of size of the local quadrature domain will affect the performance of the local weak form and it has been widely studied (Atluri and Shen, 2002, Liu, 2002; Liu and Gu, 2003).

Hence, Eq. (9) can be simplified because the integration along the internal boundary Γ_{qi} vanishes. Equation (9) can be re-written as:

$$\begin{aligned} &\int_{\Omega_q} (\widehat{w}_i m\ddot{u}_i + \widehat{w}_i c\dot{u}_i + \widehat{w}_{i,j}\sigma_{ij})\mathrm{d}x - \int_{\Gamma_{qu}} \widehat{w}_i t_i \mathrm{d}\Gamma \\ &\quad + \alpha \int_{\Gamma_{qu}} \widehat{w}_i u_i \mathrm{d}\Gamma = \int_{\Gamma_{qt}} \widehat{w}_i \bar{t}_i \mathrm{d}\Gamma \\ &\quad + \alpha \int_{\Gamma_{qu}} \widehat{w}_i \bar{u}_i \mathrm{d}\Gamma + \int_{\Omega_q} \widehat{w}_i b_i \mathrm{d}\Omega \end{aligned} \tag{11}$$

2.3 Discrete formulations and the numerical implementations

The global problem domain Ω is represented by distributed nodes. In the dynamic analysis, $\mathbf{u}$ is the function both of space co-ordinate and time. Only space domain is discretized. The moving least squares (MLS) approximation (Lancaster and Salkauskas, 1986; Belytschko et al., 1994; Liu, 2002) is used to construct meshfree shape functions. Hence, we have

$$\begin{aligned} \mathbf{u}(\mathbf{x},t) &= \begin{Bmatrix} u(\mathbf{x},t) \\ v(\mathbf{x},t) \end{Bmatrix} = \sum_{j=1}^{n} \begin{bmatrix} \phi_j(\mathbf{x}) & 0 \\ 0 & \phi_j(\mathbf{x}) \end{bmatrix} \begin{Bmatrix} u_j(t) \\ v_j(t) \end{Bmatrix} \\ &= \sum_{j=1}^{n} \mathbf{\Phi}_j(\mathbf{x})\mathbf{u}_j(t) \end{aligned} \tag{12}$$

where $\mathbf{u}(\mathbf{t})$ is the vector of nodal displacements at time t, Φ is the matrix of shape functions. Substituting Eq. (12) into the strong form Eq. (6) and the local weak form Eq. (11) for all nodes leads to the following discrete equations

$$\mathbf{M}\ddot{\mathbf{U}}(t) + \mathbf{C}\ddot{\mathbf{U}}(t) + \mathbf{K}\mathbf{U}(t) = \mathbf{F}(t) \tag{13}$$

where $\mathbf{U}$ is the vector of displacements for all nodes in the entire problem domain. $\mathbf{M}$, $\mathbf{C}$, $\mathbf{K}$ and $\mathbf{F}$ are defined as

$$\mathbf{M}_{ij} = \begin{cases} \int_{\Omega_q} m\widehat{\mathbf{w}}(\mathbf{x},\mathbf{x}_i)\mathbf{\Phi}_j(\mathbf{x})\mathrm{d}\Omega & \Omega_q(\mathbf{x}_i) \cap \Gamma_t \neq \emptyset \\ -m\mathbf{\Phi}_j(\mathbf{x}_i) & \Omega_q(\mathbf{x}_i) \cap \Gamma_t = \emptyset \end{cases} \tag{14}$$

$$\mathbf{C}_{ij} = \begin{cases} \int_{\Omega_q} c\mathbf{w}(\mathbf{x},\mathbf{x}_i)\mathbf{\Phi}_j(\mathbf{x})\mathrm{d}\Omega & \Omega_q(\mathbf{x}_i) \cap \Gamma_t \neq \emptyset \\ -c\mathbf{\Phi}_j(\mathbf{x}_i) & \Omega_q(\mathbf{x}_i) \cap \Gamma_t = \emptyset \end{cases} \tag{15}$$

$$\mathbf{K}_{ij} = \begin{cases} \int_{\Omega_q} \widehat{\mathbf{v}}_i^{\mathrm{T}}(\mathbf{x},\mathbf{x}_i)\mathbf{D}\mathbf{B}_j(\mathbf{x})\mathrm{d}\Omega - \int_{\Gamma_{qi}} \widehat{\mathbf{w}}(\mathbf{x},\mathbf{x}_i)\mathbf{N}\mathbf{D}\mathbf{B}_j(\mathbf{x})\mathrm{d}\Gamma \\ -\int_{\Gamma_{qu}} \widehat{\mathbf{w}}(\mathbf{x},\mathbf{x}_i)\mathbf{N}\mathbf{D}\mathbf{B}_j(\mathbf{x})\mathrm{d}\Gamma \\ +\alpha \int_{\Gamma_{qu}} \widehat{\mathbf{w}}(\mathbf{x},\mathbf{x}_i)\mathbf{\Phi}_j(\mathbf{x})\mathrm{d}\Gamma, & \Omega_q(\mathbf{x}_i) \cap \Gamma_t \neq \emptyset \\ \mathbf{L}^{\mathrm{T}}\mathbf{D}\mathbf{L}\Phi_j(\mathbf{x}_i) & \Omega_q(\mathbf{x}_i) \cap \Gamma_t = \emptyset \end{cases} \tag{16}$$

$$\mathbf{F}_i(t) = \begin{cases} \int_{\Gamma_{qt}} \widehat{\mathbf{w}}(\mathbf{x},\mathbf{x}_i)\bar{\mathbf{t}}(t)\mathrm{d}\Gamma + \int_{\Omega_q} \widehat{\mathbf{w}}(\mathbf{x},\mathbf{x}_i)\mathbf{b}(t)\mathrm{d}\Omega \\ +\alpha \int_{\Gamma_{qu}} \widehat{\mathbf{w}}(\mathbf{x},\mathbf{x}_i)\bar{\mathbf{u}}(t)\mathrm{d}\Gamma, & \Omega_q(\mathbf{x}_i) \cap \Gamma_t \neq \emptyset \\ \mathbf{b}(\mathbf{x}_i,t), & \Omega_q(\mathbf{x}_i) \cap \Gamma_t = \emptyset \end{cases} \tag{17}$$

with $\widehat{\mathbf{w}}(\mathbf{x},\mathbf{x}_i)$ being the value of the weight function matrix, corresponding to node i, evaluated at the point $\boldsymbol{X}$, $\mathbf{\Phi}_j$ is the matrix of shape functions, and

$$\mathbf{N} = \begin{bmatrix} n_x & 0 & n_y \\ 0 & n_y & n_x \end{bmatrix}, \quad \mathbf{B}_j(\mathbf{x}) = \begin{bmatrix} \phi_{j,x}(\mathbf{x}) & 0 \\ 0 & \phi_{j,y}(\mathbf{x}) \\ \phi_{j,y}(\mathbf{x}) & \phi_{j,x}(\mathbf{x}) \end{bmatrix} \tag{18}$$

$$\begin{aligned} \widehat{\mathbf{w}}(\mathbf{x},\mathbf{x}_i) &= \begin{bmatrix} \widehat{w}(\mathbf{x},\mathbf{x}_i) & 0 \\ 0 & \widehat{w}(\mathbf{x},\mathbf{x}_i) \end{bmatrix}, \\ \widehat{\mathbf{v}}_i(\mathbf{x},\mathbf{x}_i) &= \begin{bmatrix} \widehat{w}_{i,x}(\mathbf{x},\mathbf{x}_i) & 0 \\ 0 & \widehat{w}_{i,y}(\mathbf{x},\mathbf{x}_i) \\ \widehat{w}_{i,y}(\mathbf{x},\mathbf{x}_i) & \widehat{w}_{i,x}(\mathbf{x},\mathbf{x}_i) \end{bmatrix} \end{aligned} \tag{19}$$

$$\mathbf{L} = \begin{bmatrix} \frac{\partial}{\partial x} & 0 \\ 0 & \frac{\partial}{\partial y} \\ \frac{\partial}{\partial y} & \frac{\partial}{\partial x} \end{bmatrix}, \quad \mathbf{D} = \frac{E}{1-\nu^2} \begin{bmatrix} 1 & \nu & 0 \\ \nu & 1 & 0 \\ 0 & 0 & (1-\nu)/2 \end{bmatrix} \tag{20}$$

where $(n_x,\ n_y)$ is the unit outward normal to the boundary Γ_q,

To compute $\mathbf{M}$, $\mathbf{C}$, $\mathbf{K}$ and $\mathbf{F}$, numerical integrations are required for some field nodes. Although a part of nodes need numerical integrations that are only performed in regular-shaped local quadrature domains, attentions are

still needed to obtain the exact numerical integration. The Ω_q should be divided into small regular partitions and sufficient Gauss quadrature points should be used in each small partition. A detailed discussion of local numerical integrations can be seen in the books by Atluri and Shen (2002) and Liu (2002).

For nodes whose local quadrature domains Ω_q intersect with the natural boundaries, the local weak form is used. Therefore, as shown in Fig. 1, for a node $\mathbf{x}_i$, there exist two local domains: the local quadrature domain Ω_q of node $\mathbf{x}_i$ (size r_q) for numerical integration and the support domain Ω_s of a point $\mathbf{x}_Q$ (size r_s) for construction shape functions.

For field nodes whose local quadrature domains Ω_q do not intersect with the natural boundaries, the strong forms are used. As shown in Fig. 1, there is only one local domain: the support domain Ω_s, needed.

3 Numerical examples for 2-D elastodynamics

Several numerical examples of two-dimensional electrodynamics are studied to examine the efficiency and performance of the MWS method. The units are taken as standard international (SI) units in following examples unless specially mentioned.

3.1 A 1D truss member with derivative boundary conditions

To demonstrate the effectivity of the MWS methods, firstly consider now a mechanics problem of a truss member or bar with force (derivative) boundary conditions. The governing equation in the form of ODE is

$$EA\frac{\mathrm{d}^2u}{\mathrm{d}x^2}+b(x)=0 \tag{21}$$

where E is the Young's modulus, A is the cross-section area, u is the axial displacement in the x direction, b is the body force in x direction, and L is the length of the truss element. For simplicity, $E=1.0$, $A=1.0$, $L=1.0$. A more complex source term of non-polynomial form $b(x)=-(2.3\pi)^2\sin(2.3\pi x)$ is used in this study.

Displacement (Dirichlet) and the force (derivative) boundary condition boundary conditions are given by:

$$u|_{x=0}=0,\quad f=EA\left.\frac{\mathrm{d}u}{\mathrm{d}x}\right|_{x=L}=-2.3\pi\cos(2.3\pi x) \tag{22}$$

The exact solution of the problem can be easily obtained, which yields

$$u^{\text{exact}}(x)=-\sin(2.3\pi x) \tag{23}$$

For comparisons, the same problem can be solved by imposing the displacement (Dirichlet) boundary conditions at $x=L$ using the exact solution.

In seeking for an approximate numerical solution, the 1D truss member is represented using 11 regularly and irregularly distributed nodes, respectively. To construct meshfree shape function, 3 nearest nodes are selected in the local support (interpolation) domain. The average relative error is used as the error indicator, which is defined as

$$e=\frac{1}{N}\sum_{i=1}^{N}\frac{\left|u_i^{\text{num}}-u_i^{\text{exact}}\right|}{\left|u_i^{\text{exact}}\right|} \tag{24}$$

where u_i^{num} and u_i^{exact} are the displacement at the ith node obtained using the numerical methods and the exact solution given in Eq. (23), respectively, and N is the number of field nodes.

Table 1 lists the error in numerical results obtained using the different methods. From Table 1, we can make the following remarks.

1) If the problem is subjected only to Dirichlet boundary conditions without any derivative boundary conditions, the collocation method yields very good results.
2) The presence of the derivative boundary conditions leads to big errors in the solution. If no special treatment for the force boundary condition (the direct collocation method) is used, the error of the direct collocation method becomes 11.3%. The error magnification is more than 22 times.
3) Special treatments for handling the force (derivative) boundary conditions can improve the accuracy of the solution.
4) We can clearly see that the MWS method produces the best result for both regular and irregular nodal distributions.

This example has proven that the MWS method can improve the accuracy of the solution for a problem with the derivative boundary conditions. In this problem, the local weak form is only used for two nodes at and near the natural boundary. Although the numerical integrations are, in fact, not necessary for a 1D problem, this example can show the effectivity of the MWS method. Liu and Gu (2003) have studied the accuracy and performance of the MWS method for the 2D elasto-static problems. Very results have been obtained.

It should be also mentioned here that to obtain the result of the direct collocation method in Table 1, no special treatments for the force boundary condition is used. Hence, the computational error is relatively big. To improve the accuracy of the collocation method with

Table 1 Relative errors e (%) in results obtained different methods

Schemes	Regular nodes	Irregular nodes
Only Dirichlet BC	0.51	1.36
With derivative BC		
The direct collocation method	11.3	6.12
MWS	1.24	2.98

* A total of 11 regularly and irregularly distributed notes are used, respectively. To construct meshfree shape function, three nearest nodes are selected in the local support (interpolation) domain

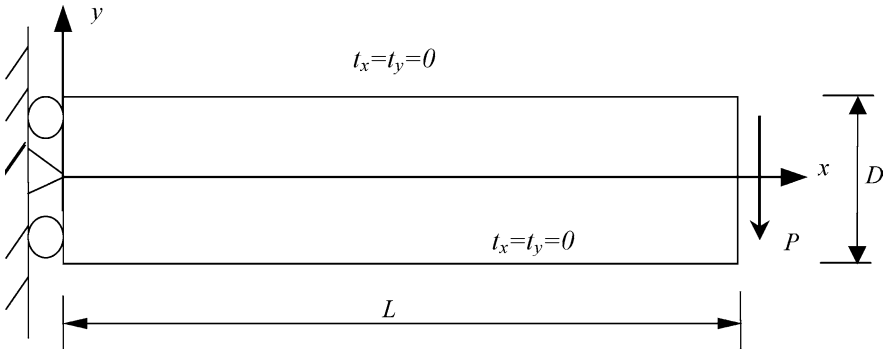

Fig. 2 A cantilever beam

the natural boundary conditions, several strategies have been developed (see e.g. Liu GR and Gu YT, 2004), e.g. using the Hermite interpolation or using suitable steep window functions (Kim and Kim, 2003) in the construction of the meshless shape function, etc.

3.2 Free vibration analysis

3.2.1 Cantilever beam

A cantilever beam shown in Fig. 2 is considered. The beam is of length L and height D subjected to a parabolic traction at the free end. The beam has a unit thickness and a plane stress problem is considered. The parameters are taken as $E = 3.0 \times 10^7$, $v = 0.3$, $D = 12$, $L = 48$, and $P = 1000g(t)$. Where $g(t)$ is the function of time t. As shown in Fig. 2, three boundaries of the beam are considered as natural boundaries.

The present MWS method is used for the free vibration analysis of a 2-D structure that is a cantilever beam, as shown in Fig. 2. The mass density of this beam is $m = 1.0$. Three kinds of nodal arrangements (55 regular nodes, 189 regular nodes and 189 irregular nodes shown in Figs. 3(a)-(b) are used. In the free vibration analyses, $\alpha_s = 3.5$ is used for the support (interpolation) domain to construct MLS shape functions. Natural frequencies of three nodal distributions obtained by the MWS method are listed in Table 2. The results obtained by the FEM commercial software package, ANSYS, using rectangular elements with the same number of nodes are listed in the same table. From this table, one can observe that the results by the present MWS method are in very good agreement with those obtained using FEM. The convergence of the present method is also demonstrated in Table 2. As the number of nodes increases, results obtained by the present MWS method approach to the FEM results with extremely fine mesh, which serves as the reference. The first three eigenmodes obtained by the MWS method are plotted in Fig. 4. Comparing with FEM (ANSYS) results, almost identical results are obtained.

Frequencies results of irregular 189 nodes are also listed in Table 2. From this table, one can observe that very good results are obtained using the irregular distribution nodal arrangement. The computational

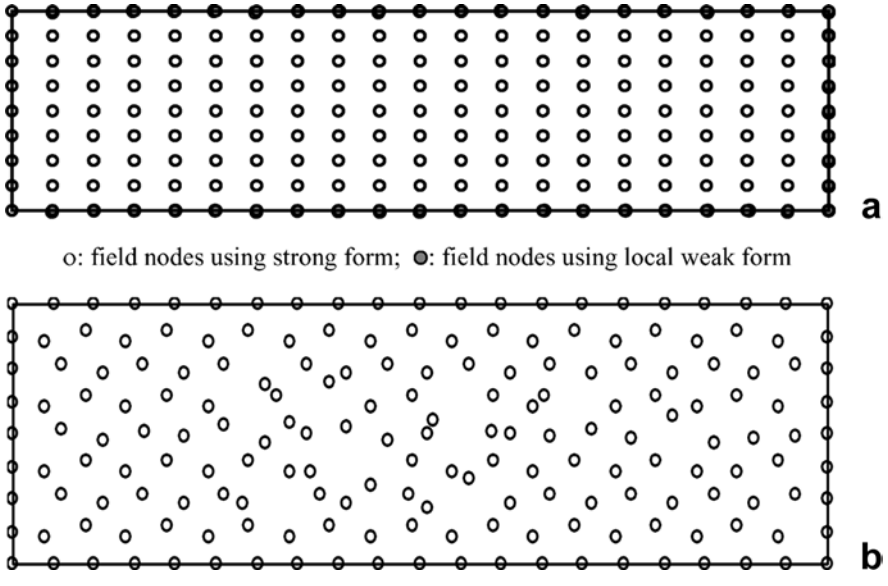

Fig. 3 Distribution of nodes for cantilever beam. **(a)** 189 regular nodes; **(b)** 189 irregular nodes

Table 2 Natural frequency of a cantilever beam with different nodal distributions

Mode	55 nodes		189 nodes			Reference
	MWS	FEM	MWS (regular nodes)	MWS (irregular nodes)	FEM (ANSYS)	FEM (4850 DOF*) (ANSYS)
1	26.7693	28.60	27.8370	27.7909	27.76	27.72
2	141.3830	144.12	141.1300	141.3111	141.79	140.86
3	179.7013	179.77	179.9077	179.9932	179.82	179.71
4	327.0243	328.47	323.8497	323.0334	328.01	323.89
5	527.3999	523.36	522.3307	522.7783	534.23	523.43
6	539.0598	532.41	537.1464	537.4757	538.08	536.57
7	730.1131	716.35	727.2628	727.5968	751.15	730.04
8	886.5635	859.23	881.5703	881.7091	887.69	881.28
9	896.9009	875.84	896.1059	897.2380	920.36	899.69
10	1004.7952	956.34	997.7824	998.1700	1022.78	1000.22

*DOF—degree of freedom

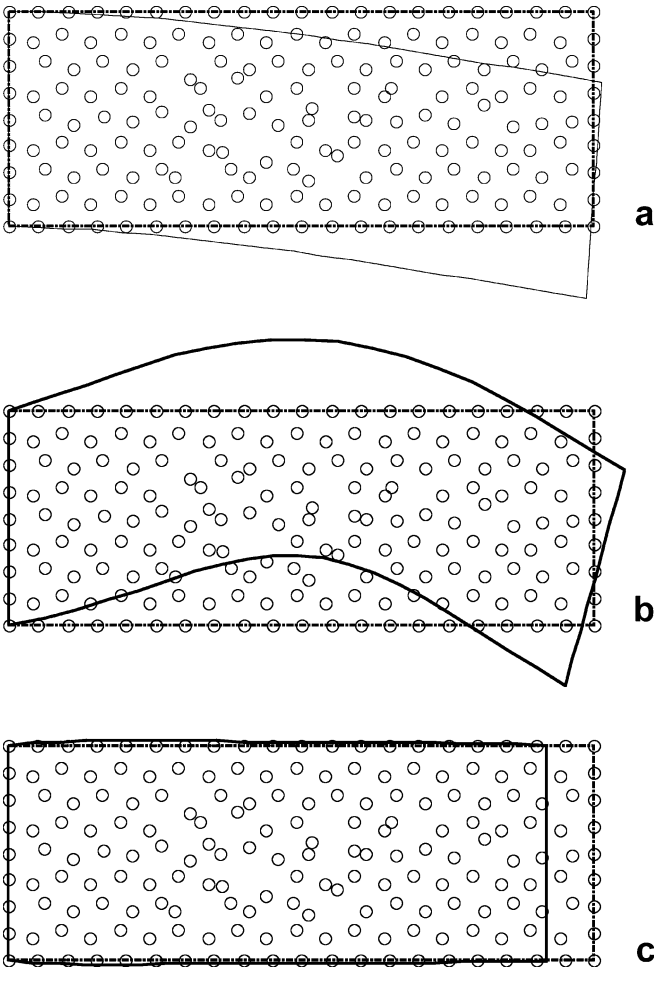

Fig. 4 Eigenmodes for the cantilever beam by the MWS method using 189 irregular nodes. (a) Mode 1; (b) Mode 2; (c) Mode 3

stability and high accuracy for a non-structured nodal distribution are very significant advantages of the present MWS method. These properties are very beneficial for practical applications of the MWS method.

3.2.2 A variable cross-section beam

In this example the present MWS method is used for free vibration analysis of a cantilever beam with variable cross-sections, shown in Fig. 5. Results are obtained for following numerical parameters: the length $L = 10$, the height $h(0) = 5$, $h(L) = 3$, the thickness $t = 1.0$, $E = 3.0 \times 10^7$, $v = 0.3$ and $m = 1.0$. The nodal arrangement is shown in Fig. 5. Results obtained by the presented MWS method and the FEM software package, ABAQUS, are listed and compared in Table 3. Results obtained by these two methods are in good agreement.

3.3 Forced vibration analysis by MWS

The methods of solving the Eq. (13) of the forced vibration analysis can be largely divided into two categories: the modal analysis and the direct analysis. The direct analysis methods are utilized in this paper. Several direct analysis methods have been developed to solve the dynamic Eq. (13), such as central difference method and Newmark method (e.g., Gu and Liu, 2001b). The Newmark method is an unconditionally stable provided

$$\delta \geq 0.5 \text{ and } \beta \geq \frac{1}{4}(\delta + 0.5)^2 \tag{25}$$

It has been found that $\delta = 0.5$ and $\beta = 0.25$ leads to acceptable results for most of problems. Hence, the Newmark method with $\delta = 0.5$ and $\beta = 0.25$ is used in this paper.

The forced vibration for a 2-D structure, a cantilever beam, as shown in Fig. 2, is analyzed. The parameters are taken as the same as the example in section 3.2.1. For simplification, the mass density of this beam is $m = 1.0$. In this numerical example for the forced vibration analysis, the beam subjected to a parabolic traction at the free end, $P = 1000g(t)$. $g(t)$ is the function of time. Two functions of time, $g(t)$, as shown in Fig. 6, are considered. As shown in Fig. 3 (a), 189 uniformed nodes are used to discretize the problem domain.

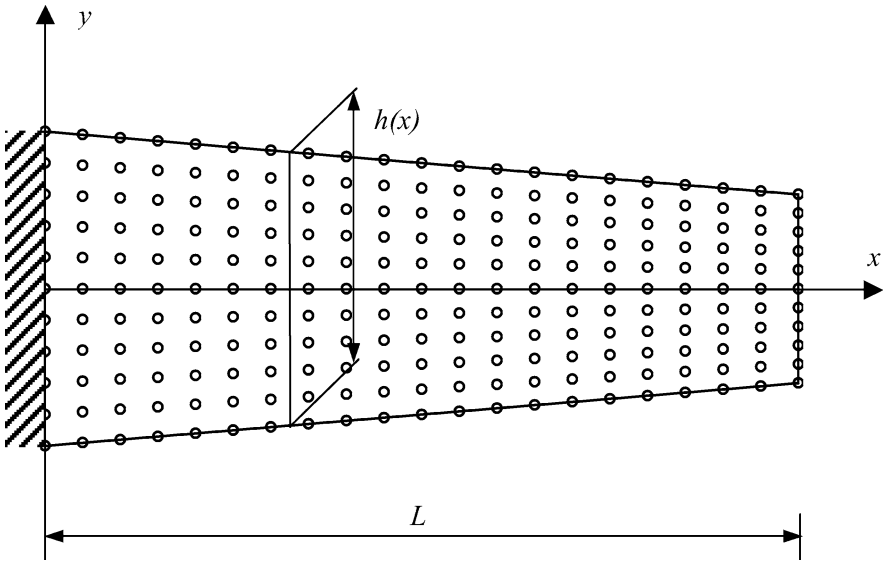

Fig. 5 A cantilever beam with variable cross-sections and the nodal distribution

Table 3 Natural frequencies of a variable cross-section cantilever beam

Modes	$\omega(rd/s)$			
	1	2	3	4
MWS method	263.14	924.97	954.13	1857.26
FEM (ABAQUS)	262.09	918.93	951.86	1850.92

Displacements and stresses for all nodes are obtained. Detailed results of vertical displacement, u_y, on the middle node at the free end of the beam are presented.

3.3.1 Dynamic relaxation

If $g(t)$ is a constant 1.0, as shown in Fig. 6(a), the dynamic analysis is so-called dynamic relaxation. In this problem, a constant loading is suddenly loaded to this structure, and then the loading will keep unchanged. If the damping is neglect, it will become a steady harmonic vibration with the static deformation (given by the static analysis) as the equilibrium position. If the damping is considered, the response will converge to the static deformation. Hence, using the above properties, the dynamic relaxation can be used to check the stability and efficiency of a numerical method for the dynamic analysis.

The present MWS method is used to perform the dynamic relaxation analysis. In this analysis, the time step, $\Delta t = 4 \times 10^{-3}$, is used. The response of $c = 0$ is firstly obtained. It has found that it is a stable vibration with the static deformation, whose analytical solution (Timoshenko and Goodier, 1970; Liu, 2002) is $u_y = 0.0089$, as the equilibrium position.

Results for $c = 0.4$ are then obtained. Table 4 lists results of several time steps at $t \approx 50$s. It can be found that the MWS method gives very stable and convergent results. Figure 7 shows the results for $c = 0.4$. It can be found that the response converges to $u_y = 0.008843$. Compared with the exact static solution, the error is only about 0.5%. Hence, it demonstrates that the present MWS method works well for the forced vibration analysis.

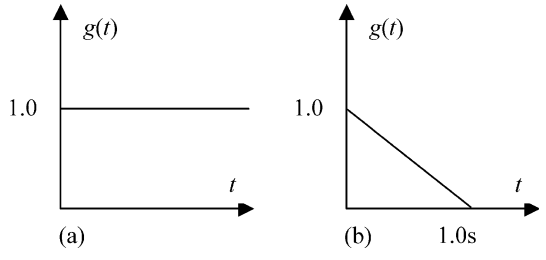

Fig. 6 Two different time function $g(t)$

3.3.2 Transient response

The transient response of the beam subjected to a suddenly loaded and suddenly vanished force $P = 1000g(t)$ is considered. The function $g(t)$ is shown in Fig. 6(b). The present MWS method is used to obtain the transient

Table 4 Results of several time steps near **t** = 50s

No. of time step	Time (s)	Displacement u_y
11750	0.470000E + 02	−0.00883283
11875	0.475000E + 02	−0.00883255
12000	0.480000E + 02	−0.00883264
12125	0.485000E + 02	−0.00882592
12250	0.490000E + 02	−0.00883220
12375	0.495000E + 02	−0.00884123
12500	0.500000E + 02	−0.00884174

Exact: $u_y = -0.0089$

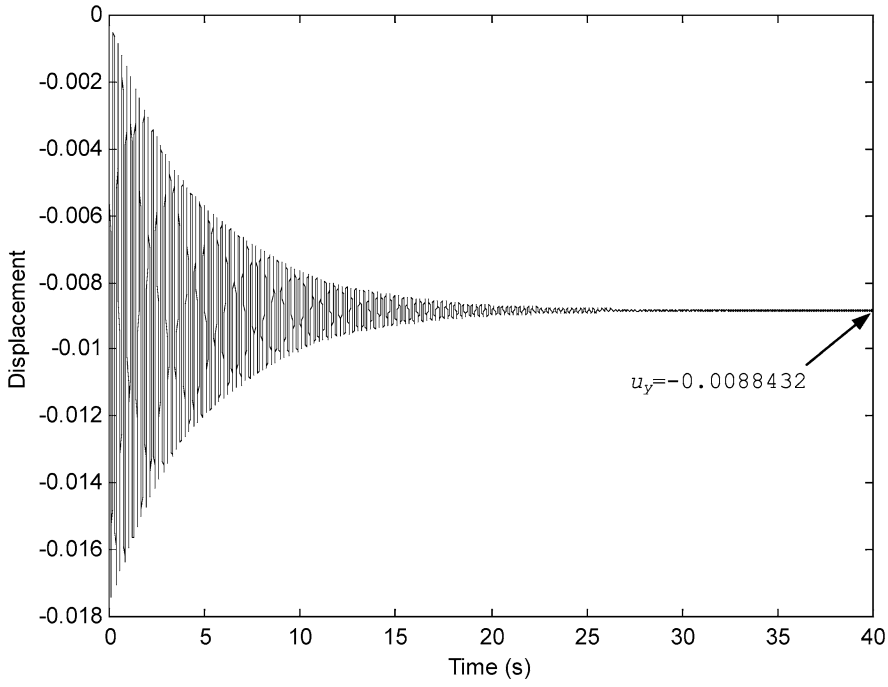

Fig. 7 Displacements u_y at the middle of the free end of the beam for constant $g(t)$ (damping $c = 0.4$)

response with and without damping. The Newmark method is utilized in this analysis. The result for $c = 0$ is plotted in Fig. 8. Many time steps are calculated to examine the stability of the presented MWS formulation and code. From Fig. 8, one can observe that the response becomes a stable vibration after 1.0 s. A very stable result is obtained by the MWS method.

The result for $c = 0.4$ is plotted in Fig. 9. From Fig. 9, one can observe that the amplitude of the vibration decrease with time because of damping. Again, a very stable and accurate result is obtained.

4 Numerical results for a MEMS device

In order to demonstrate validity of the present MWS method, the dynamics behavior of a typical MEMS device is simulated. The MEMS device is simplified as a

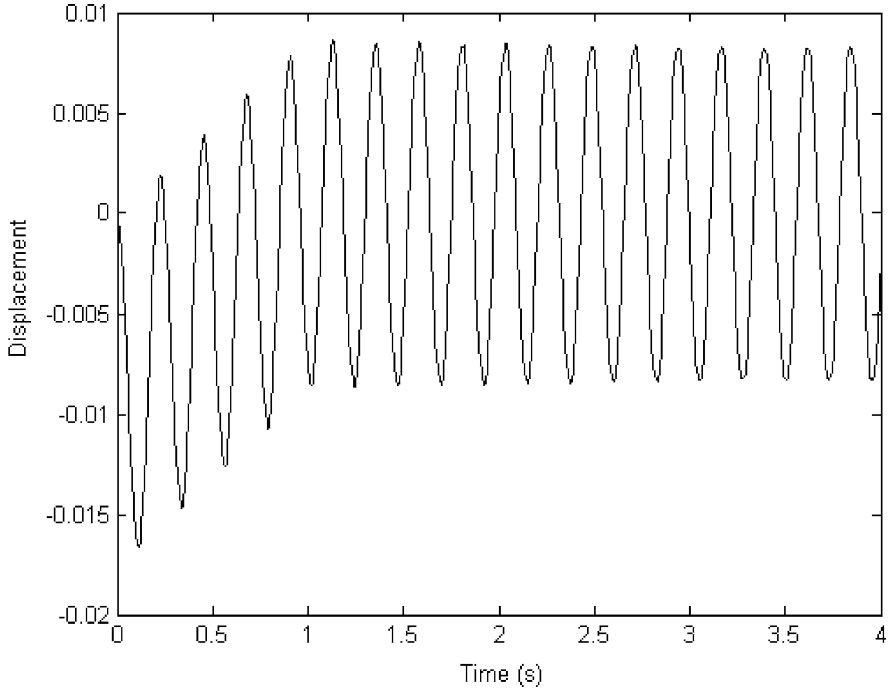

Fig. 8 Transient displacements u_y at the middle of the free end of the beam for $g(t)$ in Figure 6(b)

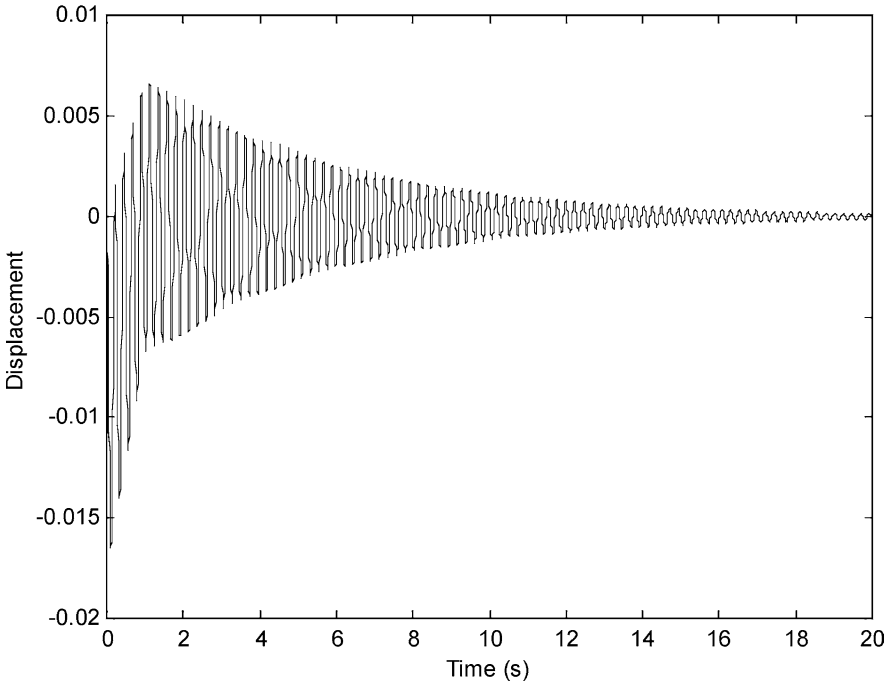

Fig. 9 Transient displacements u_y the middle of the free end of the beam for $g(t)$ in Figure 6(b) using Newmark method (damping, $c = 0.4$)

fixed-free thick beam, shown in Fig. 10. Hence, there are derivative boundary conditions at the free end of the device. The MWS formulation can be easily obtained using the governing equations of thick beam (Reddy, 1993) and the similar algorithm in Sect. 2.

The dimension size of the device is: 80 μm long, 10 μm wide and 0.5 μm thick. At the initial time, the gap between the device and the bottom electrode is 0.7 μm. The Young's modulus is 169 GPa, and the mass density is 2231 kg/m^3. The work principle of the MEMS device is: when the applied voltage imposes on the device, it will deform. With the increasing of the applied voltage, the deflection of the device increases. When the applied voltage reaches one certain value defined as the critical pull-in voltage, the device becomes unstable and the centre of it touches the bottom electrode. Induced by the applied voltage, the MEMS will be subjected to a non-linear dynamic loading, f (Li et al. 2003), and it takes the following form

$$f = -\frac{\varepsilon_0 \tilde{V}^2 \tilde{w}}{2g^2}\left(1 + 0.65\frac{g}{\tilde{w}}\right) \tag{26}$$

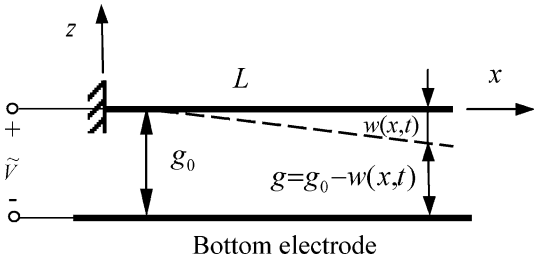

Fig. 10 The MEMS device simplified as fixed-free thick beam

where ε_0 is the permittivity of vacuum, $\tilde{V}$ applied voltage, $\tilde{w}$ beam width, and g the gap between the beam and bottom electrode, $g = g_0 - w(x,t)$, where g_0 is the distance between the beam and electrode before the beam deflects, as shown in Fig. 10, and $w(x,t)$ is the device deflection.

Equation (26) shows that the loading is also a function of the deflection. The MWS system equation for this problem, therefore, is a nonlinear dynamic equation. An iteration technique is required in each time step.

In this dynamic simulation, the time step is taken as $\Delta t = 5 \times 10^{-3}$μs. The peak deflection, which is at the right end of the cantilever beam, under different applied voltages is studied, as shown in Fig. 11. From the figure, it is can be found that the peak deflection of the beam increases nonlinearly as the applied voltage increases. The fundamental frequency of the cantilever beam decreases with the increase of the applied voltages. The dynamic critical pull-in voltage for the cantilever beam is 2.13 volt that agrees very well with the results of 2.12 volt obtained by Li et al. (2003). This example shows that the MWS method leads to very stable and accurate results for the simulation of the MEMS device under the non-linear dynamic loading.

5 Discussion and conclusions

A meshfree weak-strong (MWS) form method is developed for dynamic analyses of time dependent problems. In the MWS method, both the strong and local weak forms are used. The strong form or collocation method is used for all nodes whose local quadrature domains do not intersect with natural (derivative) boundaries. There

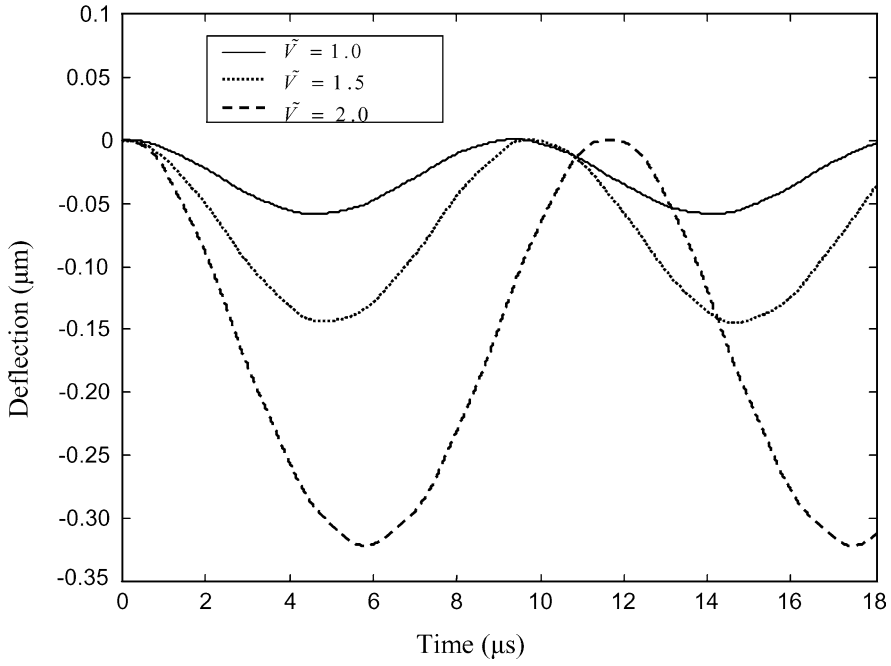

Fig. 11 Dynamic response of the MEMS devices under different applied voltages

is no requirement for numerical integrations for these nodes. The local weak form is only used for nodes on or near the natural boundaries. The natural boundary conditions can then be easily imposed to produce stable and accurate solutions. The MWS method is used for analyses of free vibration and forced vibration of 2-D structures as well as the non-linear dynamic performance of the MEMS device. Numerical examples have demonstrated the effectiveness of the present MWS method for the time dependent problems.

It can conclude that the present MWS method takes fully the advantages of meshfree strong-form methods and meshfree weak form methods. Therefore, it is efficient, accurate and stable. In the same time, it requires the least mount of mesh in the entire computation process, compared with all the meshfree weak form methods developed so far. As an efficient meshfree method, the present MWS method has a good potential for solving linear and non-linear time dependent problems.

References

1. Atluri SN, Kim HG, Cho JY (1999) A critical assessment of the truly meshless local Petrov-Galerkin (MLPG), and local boundary integral equation (LBIE) methods. Comput. Mech. 24:348–372
2. Atluri SN, Shen SP (2002), The Meshless Local Petrov-Galerkin (MLPG) method. Tech Science Press. Encino USA
3. Belytschko T, Lu YY, Gu L (1994) Element-free Galerkin methods. Int. J. Numer. Meth. Eng. 37:229–256
4. De S, Bathe KJ (2000) The method of finite spheres. Comput. Mech. 25:329–345
5. Gu YT, Liu GR (2001a) A meshless Local Petrov-Galerkin (MLPG) formulation for static and free vibration analysis of thin plates. Computer Modeling in Engineering & Sciences (CMES) 2(4):463–476
6. Gu YT, Liu GR (2001b) A meshless local Petrov-Galerkin (MLPG) method for free and forced vibration analyses for solids. Comput. Mech. 27:188–198
7. Gu YT, Liu GR (2001c) A local point interpolation method for static and dynamic analysis of thin beams. Comput. Meth. Appl. Mech. Eng. 190:5515–5528
8. Kim DW, Kim Y (2003) Point collocation methods using the fast moving least-square reproducing kernel approximation. Int. J. Numer. Meth. Eng. 56:1445–1464
9. Lam KY, Wang QX, Hua Li (2004) A novel meshless approach – Local Kriging (LoKriging) method with two-dimensional structural analysis, Comput. Mech. 33:235–244
10. Lancaster P , Salkauskas K (1986) Curve and surface fitting, an introduction. Academic Press
11. Li Hua, Wang QX , Lam KY, (2004) Development of a novel meshless Local Kriging (LoKriging) method for structural dynamic analysis Comput. Meth. Appl. Mech. Eng. 193(23–26):2591–2611
12. Li Hua, Wang QX , Lam KY (2003), A variation of local point interpolation method (vLPIM) for analysis of microelectro-mechanical systems (MEMS) device. Engineering Analysis with Boundary Elements(in press)
13. Liu GR (2002), Mesh Free Methods: Moving Beyond the Finite Element Method. CRC press, Boca Raton, USA
14. Liu GR , Gu YT (2003), A meshfree method: Meshfree Weak-Strong (MWS) form method,for 2-D solids. Comput. Mech. 33(1):2–14
15. Liu GR , Gu YT (2004), An Introduction to MFree Methods and Their Programming. Kluwer Academic Publishers (in press)
16. Liu GR , Gu YT (2001a) A point interpolation method for two-dimensional solids. Int. J. Numer. Meth. Eng. 50:937–951
17. Liu GR , Gu YT (2001b) A local point interpolation method for stress analysis of two-dimensional solids. Struct. Eng. Mech. 11(2):221–236
18. Liu GR , Gu YT (2001c) A local radial point interpolation method (LR-PIM) for free vibration analyses of 2-D solids. J. Sound Vibration 246(1):29–46
19. Liu GR , Yan L, Wang JG and Gu YT (2002) Point interpolation method based on local residual formulation using radial basis functions. Struct. Eng. Mech. 14(6):713–732

20. Reddy JN (1993) An introduction to the Finite Element Method. New York: McGraw Hill, 2nd edition
21. Zhu T, Zhang JD , Atluri SN (1998) Local boundary integral equation (LBIE) method in computational mechanics, and a meshless discretization approach. Comput. Mech. 21(3):223–235
22. Timoshenko SP , Goodier JN (1970), Theory of Elasticity. 3rd Edition, McGraw-hill, New York
23. Wang JG , Liu GR (2002) A point interpolation meshless method based on radial basis functions. Int. J. Numer. Methods. Eng. 54:1623–1648
24. Zhang X, Liu XH, Song KZ , Lu MW (2001) Least-square collocation meshless method. Int. J. Numer. Methods. Eng. 51(9):1089–1100